# Pressure Effects on Columnar Lyotropics: Anisotropic Compressibilities in Guanosine Monophosphate Four-Stranded Helices

**Pamela Ausili,[†] Michela Pisani,[†] Stephanie Finet,[‡] Heinz Amenitsch,[§] Claudio Ferrero,[‡] and Paolo Mariani*,[†]**

*Istituto di Scienze Fisiche and INFM, Università di Ancona, Via Ranieri 65, I-60131 Ancona, Italy, European Synchrotron Radiation Facility, BP 220, F-38043 Grenoble Cedex, France, Sincrotrone Trieste S.C.p.A., Strada Statale 14, km 163.5, I-34016 Basovizza (Trieste), Italy, and Institute of Biophysics and X-ray Structure Research, Austrian Academy of Sciences, Graz, Austria*

*Received: September 22, 2003*

Guanosine in water self-associates into stable structures, made by four-stranded helices composed of stacked guanosine tetramers. High-pressure synchrotron X-ray diffraction was used to investigate helix stability and energetics in the hexagonal phase. An unusual lateral interhelix negative compressibility was found, indicating that a redistribution of water inside the cell occurs during compression and enforcing the original hypothesis that in guanosine phases water separates into different regions. Moreover, changes in free energy were calculated, and helix elastic constants were derived.

## Introduction

Self-recognition and self-assembly processes lead to the formation of complex supramolecular structures from simple molecules. An important case concerns guanine, which, unique among the nucleic acid bases, forms a variety of non-B-DNA conformations such as quadruplex structures.[1−5] This property is related to the arrangement of H-bond donor and acceptor groups in guanine, is essential for genome integrity, and appears to play an important role in cellular aging and cancer.[5,6] The self-assembling process, which is specifically favored by monovalent cations that fit well in the cavities between tetrads (as Na, K, $NH_4$),[1,5,7] is illustrated in Figure 1: planar tetramers (G tetrads) result from the assembling of four guanines in a Hoogsteen-bonded fashion,[2] and four-stranded helices form by the regular stacking of tetramers. Note that tetrads are stacked perpendicular to the column axis at a typical distance of 3.3 Å (the same distance between base pairs in DNA) and are rotated with respect to each other by about 30°.[3,5,8,9] As a function of concentration, helices have been recognized to lead in water to columnar lyotropic hexagonal-type (H) and cholesteric-type (Ch) phases, whose structures were studied in detail.[3,8,9,10] As general result, the phase behavior was observed to show a strong sensitivity to the nature and concentration of counterions.[3,10]

Interactions and aggregation mechanisms of helical biomolecules were the subject of quite intensive theoretical work. Recent achievements refer in particular to the condensation properties of helical biomolecules, to the effects of counterions on their polymorphic behavior, to the rearrangement of adsorbed ions on their surfaces, and to the relationships between helical symmetry and the interplay between intermolecular repulsive and attractive forces.[11] Even if most of them are related to DNA, the analyses and the general statements were suitable to rationalize the interactions and phase behavior of a wide range of charged helical biomolecules.[12] In this context, guanosine helices were detected to obey the symmetry laws for interaction between helical macromolecules, and a balance between medium-range attraction, which induces the self-assembly, and short-range hydrational repulsion, which prevents contact between helices, was observed to be implied in condensation.[13] For the particular case of guanosine 5′-monophosphate, sodium salt (GMP), it was suggested that helices have a constant, finite length (with an average tetramer aggregation number of 70) so that the lateral force balance leads to a preferential hydration effect during swelling (i.e., the lateral and end-to-end axial interparticle distances do not change uniformly).[8,14] A schematic representation of the finite GMP helices packed in the hexagonal lattice is reported in Figure 2.

To address questions related to the mechanical properties of guanosine and four-stranded helices and the roles of preferential hydration and lateral forces on the energetic of these systems, we report in this paper on a high-pressure X-ray diffraction analysis of the structural properties of GMP helices in the hexagonal phase in the presence and absence of KCl. It has in fact been demonstrated that high pressure is a suitable thermodynamic variable for determining the structural properties and stability of lyotropic mesophases.[15,16] During compression, amphiphilic molecules (including DNA[16]) adapt to volume restriction by changing their conformation and packing: because a delicate balance of competing energetic contributions is involved in the stabilization of biological structures, such small changes in conformation can determine large structural transformations that can be easily monitored by X-ray diffraction techniques.

## Material and Methods

Hydrated samples were prepared by mixing the GMP, sodium salt (Sigma, 99% purity) with the required quantities of freshly bidistilled water or aqueous KCl solution (1 and 2 M). Final mixtures (GMP weight fractions *c* ranging from 0.9 to 0.5) were left for at least 2 days at 25 °C to avoid inhomogeneity.

* Corresponding author. E-mail: mariani@alisf1.unian.it.
[†] Università di Ancona.
[‡] European Synchrotron Radiation Facility.
[§] Sincrotrone Trieste S.C.p.A. and Austrian Academy of Sciences.

10.1021/jp036829s CCC: $27.50 
Published on Web 01/09/2004

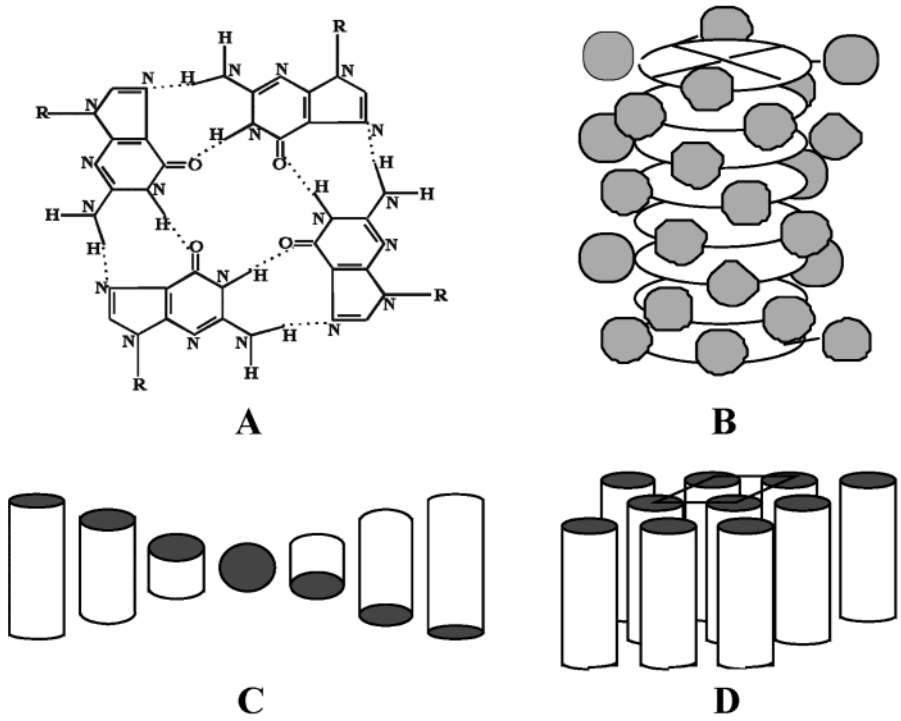


**Figure 1.** Structural models for the guanosine self-assembling. (A) Arrangement of the guanine quartet in the Hoogsteen mode. (B) Structure of the four-stranded helix: disks represent the tetramers, and gray circles indicate the sugar residue. The stacking is helical. (C) Cholesteric and (D) hexagonal arrangements of the helices, represented as cylinders.

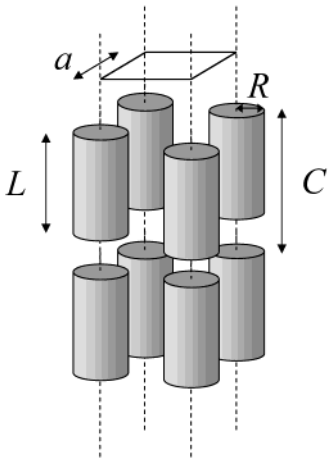


**Figure 2.** Schematic representation of the finite GMP helices packed in the hexagonal lattice. Helices are represented as finite cylinders, lined along their axes, represented by dashed lines. The 2D hexagonal unit cell is also indicated. *a* is the 2D hexagonal unit cell dimension (i.e., the lateral interaxial distance between the helices), *C* is the average distance between the lined cylinders in the axial direction, *R* is the radius of the helices, and *L* is their average length.

From the nominal composition, the GMP volume fraction $c_v$ was determined using

$$c_v = \frac{c}{c + (1 - c)(\nu_{wat}/\nu_{GMP})} \quad (1)$$

where $\nu_{GMP}$ and $\nu_{wat}$ are the specific volumes of GMP and water, respectively. For high-pressure data, volume concentrations were corrected by considering the pressure dependence of the densities reported in ref 17.

Diffraction experiments were performed at the SAXS beamline at ELETTRA Synchrotron (Trieste, Italy) with $\lambda = 1.54$ Å and $0.03 < Q < 0.6$ Å$^{-1}$ and at the ID02 beamline at ESRF (Grenoble, France) with $\lambda = 0.995$ Å and $0.016 < Q < 0.6$ Å$^{-1}$ ($Q = (4\pi\sin\theta)/\lambda$, where $2\theta$ is the scattering angle). An additional wide-angle X-ray scattering detector was used at ELETTRA to monitor diffraction patterns in the *Q* range from 0.7 to 2.5 Å$^{-1}$.

Pressure cells with diamond windows, which allow the measurement of diffraction patterns at hydrostatic pressures up to 3 kbar, were used. Particular care has been taken to check for radiation damage and for equilibrium conditions. Measurements were repeated several times at the same constant pressure to account for stability in the position and intensity of Bragg peaks. Accordingly, samples were gently compressed at a rate of 0.5−2 bar/s to ensure the onset of equilibrium conditions. The diffraction patterns were collected at 25 °C. Note that no water loss was detected before the hydrated mixtures were mounted into the pressure cell. Moreover, after the X-ray scattering experiments, the water composition of each sample was checked again by gravimetric analysis. The difference between the nominal concentration and the one measured after the pressure cycle was detected to be in the limit of the experimental errors.

## Results

GMP/water samples, prepared at different water concentrations and ionic strengths, were analyzed by X-ray diffraction as a function of the mechanical pressure. In each experiment, a number of reflections were observed, and their spacings were measured following the usual procedures.[3] Typical X-ray diffraction patterns are reported in Figure 3: in the low-angle region, from 2 to 5 peaks (depending on sample concentration) are observed, and the wide-angle region is characterized by the presence of a narrow band only. At all of the investigated conditions, the spacings of the low-angle peaks were unambiguously indexed in a 2D hexagonal lattice, and then the unit cell dimension, *a*, was derived as a function of the different experimental parameters. (Note that in the same diffraction

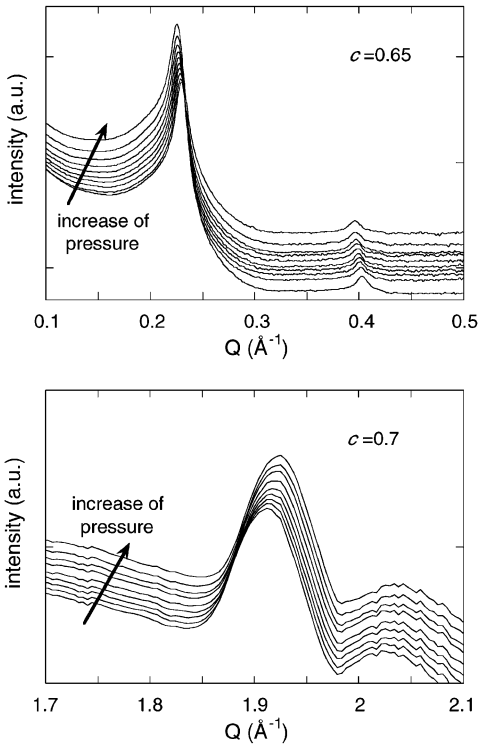


**Figure 3.** X-ray diffraction profiles obtained from GMP samples in water. (Top) Low-angle profile, $c = 0.65$. (Bottom) High-angle profile, $c = 0.7$. Spectra, measured at the Elettra Synchrotron from 1 to 1800 bars, are shown every 200 bars.

region, a diffuse band would indicate the presence of the cholesteric phase.[3]) The high-angle narrow band is the fingerprint of the columnar nature of the H phase;[3] this reflection is indeed related to the tetramer stacking,[3,8] and from its position, the distance between the neighboring tetrads, *b*, can be obtained. It should be also observed that no extra peaks were observed in the diffraction profile, indicating the absence of smecticlike order. (No long-range column−column correlation of the tetramer position exists.)

Two main features emerge from the X-ray data: the absence of phase transitions in the investigated concentration/pressure range and the pressure dependence of the positions of the observed peaks. Some quantitative results obtained in pure water are reported in Figure 4: at all concentrations, the interaxial distance increases as a function of pressure, but the tetramer repeat distance decreases. As shown in Figure 5, similar behavior is detected when samples are prepared in KCl solutions; however, the hexagonal cells appear to be slightly reduced, and the tetramer stacking distance is increased. Both effects can be easily explained. The first one is clearly related to the increased ionic strength of the aqueous medium, which reduces the lateral interhelix electrostatic repulsive forces.[13] The second effect can be associated with a Na/K ion exchange from the solution to the helices because of the highly specific affinity of the larger K ions for the cavity between the tetramers.[1,7,14]

As shown in Figures 4 and 5, *a* versus pressure data show rather linear behavior: a linear fit to the hexagonal lattice dimensions has then been used to calculate the unit cell pressure dependence, d*a*/d*P*. The results, reported in Figure 6, are significantly different from those observed in other lyotropic phases. In particular, lipidic direct hexagonal phases (that from a structural point of view are the most similar to the columnar phase here described) show *negative* d*a*/d*P* values (as well as on the order of a few tenths of an angstrom per kilobar; values

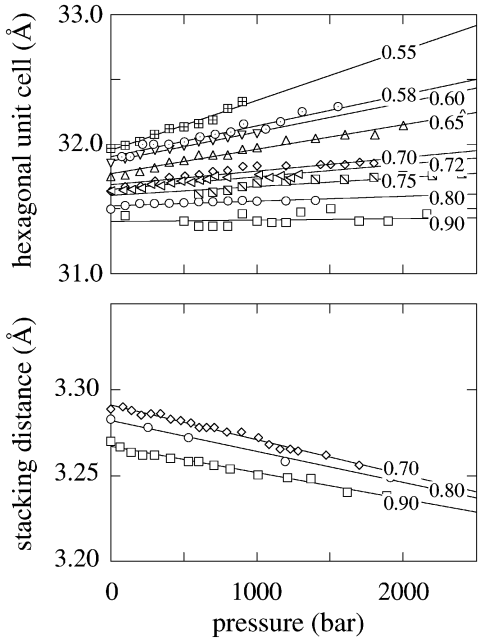


**Figure 4.** Pressure dependence of the 2D hexagonal unit cell (top frame) and of the tetramer repeat distance (lower frame) as obtained in pure water. GMP concentrations are indicated in the graph. Lines are guides for the eye.

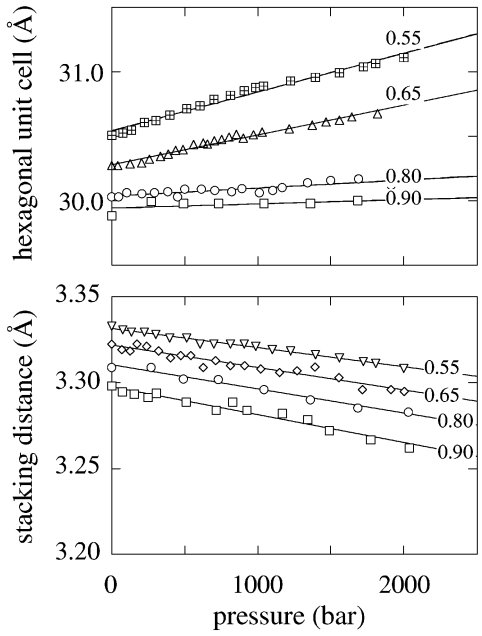


**Figure 5.** Pressure dependence of the 2D hexagonal unit cell (top frame) and of the tetramer repeat distance (lower frame) as obtained in 2 M aqueous KCl solutions. GMP concentrations are indicated on the graph. Lines are guides for the eye.

around −0.2 Å kbar$^{-1}$ were detected both in dodecyl-trimethyl-ammonium chloride and in lyso-oleoyl-phosphatidyl choline water mixtures[18]). *Positive* values were by contrast detected in inverse lipidic phases:[15,18−20] in these systems, d*a*/d*P* values ranging from 1.6 to 4 and 4 to 10 Å kbar$^{-1}$ were measured in the hexagonal[15,20] and in the most complex cubic bicontinuous phases,[15,19] respectively. Such a rather impressive dependence has been explained by considering that pressure mainly affects the lipid chain-order parameter.[19,20] Changes in lipid conformation determine a change in the basic geometrical shape of the molecules, affecting both the curvature of the lipid monolayer

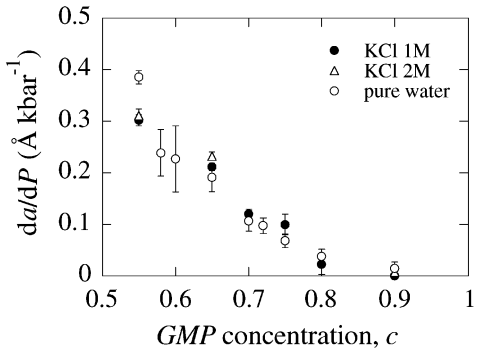


**Figure 6.** Concentration dependence of d$a$/d$P$ values obtained by a linear fitting of the hexagonal unit cell data measured as a function of pressure (see Figures 4 and 5).

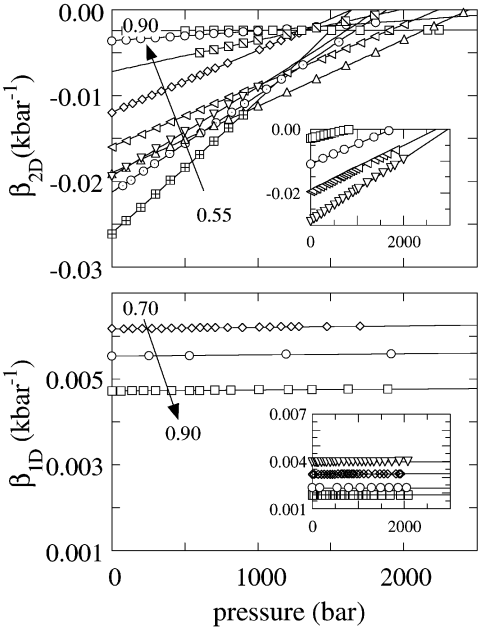


**Figure 7.** Pressure dependence of the 2D ($\beta_{2D}$, top frame) and 1D ($\beta_{1D}$, lower frame) compressibilities as obtained in pure water. The insets show compressibilities in 1 M KCl. Symbols are the same as in Figures 4 and 5; the changes in GMP concentrations are indicated by the arrows. Lines are guides for the eye.

and the hydration level of the polar head and then strongly modifying the unit cell dimensions.

From structural data, axial (1D) and lateral (2D) compressibilities, $\beta_{1D} = -1/b$ (d$b$/d$P$) and $\beta_{2D} = -1/\sigma$ (d$\sigma$/d$P$) (where $\sigma = a^2(\sqrt{3}/2)$), were calculated. The results are reported in Figure 7 and deserve for some comment. First, lateral compressibilities are negative, largely dependent on water concentration but independent of ionic strength. Second, stacking compressibilities are positive, rather small (as compared with water data, which are on the order of 0.045 to 0.03 kbar$^{-1}$ [17]), and dependent on KCl concentration.

## Discussion

High-pressure X-ray diffraction experiments on guanosine four-stranded helices in the hexagonal phase show an unusual structural behavior (Figures 4 and 5): during compression, the interhelical lateral distance increases, and the tetramer stacking distance decreases. From these data, axial and lateral compressibilities, as shown in Figure 7, have been calculated. Lateral compressibilities are negative and for increasing concentrations converge to very low (yet negative) values. Because experiments are performed at constant concentration, this suggests that during compression a change in the local sample composition occurs - a redistribution of water from the axial to the lateral interhelical region takes place (see the structural model in Figure 2). This is confirmed by the $\beta_{2D}$ dependence on water concentration. It should also be observed that the lateral compressibilities measured at different ionic strengths are rather similar, suggesting that the role played by electrostatic forces could be not primary. On the contrary, stacking compressibilities show a clear dependence on KCl concentration: in the presence of KCl, the aggregate rigidity increases, probably in relation to the preferential location of K ions from the solution to the cavity between guanine tetrads.

The nature of the observed pressure effects can be analyzed by considering that the application of pressure should push the system toward the state occupying the smallest volume. Assuming a model of rodlike particles of constant cross-sectional radius $R = 13.5$ Å[3,10] and average length $L$ packed in a 2D hexagonal cell, the 3D cell volume can be described by

$$V_{\text{cell}} = Ca^2\frac{\sqrt{3}}{2} = \frac{L\pi R^2}{c_v} \tag{2}$$

where $C$ is the average distance between the rod centers in the axial direction, normal to the 2D hexagonal cell plane (see the scheme in Figure 2). Note that the ratio $L/C$ gives essentially the fraction of water in the axial direction. The net 3D cell volume change, $\Delta V = V_{\text{cell}} - V_0$ (in the following, the index 0 refers to data at ambient pressure), which includes the changes in the partial volume of the water and the changes in the partial volume of the solute as well as any change in the interstitial volume owing to interactions of the solute with the solvent,[21] can then be calculated as a function of pressure. Because of the independence on $L$ and $C$, we will conveniently define a volume change per guanosine residue, $\Delta V^*$ (in mL mol$^{-1}$):

$$\Delta V^* = \frac{\Delta V\, 10^{-24}\aleph}{4n} = \frac{0.602\pi R^2}{4}\left(\frac{b}{c_v} - \frac{b_0}{c_{v,0}}\right) \tag{3}$$

where $\aleph$ is Avogadro's number, $n$ is the average number of stacked tetrads ($L = nb$), and the coefficient 4 accounts for the tetrameric arrangement. The same model is useful to calculate the amount of water redistributed during compression. In particular, the number of water molecules released from the axial to the lateral interhelix region per guanosine residue, $\Delta N^*$ (the star indicates that it is also independent of the helix length), is

$$\Delta N^* = \frac{b}{4V_{\text{wat}}}\left(\frac{\pi R^2}{c_v} - a^2\frac{\sqrt{3}}{2}\right) - \frac{b_0}{4V_{\text{wat},0}}\left(\frac{\pi R^2}{c_{v,0}} - a_0^2\frac{\sqrt{3}}{2}\right) \tag{4}$$

where $V_{\text{wat}}$ is the molecular volume of water. Figure 8 shows the pressure dependence of $\Delta V^*$ and $\Delta N^*$. As expected, volume variations are negative and become larger at the higher hydrations, where the amount of removed water is consistently larger.

Pressure-induced volume reduction effects have been reported for DNA on the basis of melting experiments.[16,22] Hydrostatic pressure has in fact been proven to stabilize the double helices against thermal denaturation, and pressure-induced better (and closer) base stacking (in particular, of the bases located at the ends of the helices, which are expected to be less stable) has been invoked to explain such behavior.[22] This is opposite to the situation in most biological systems, where increased hydrostatic pressure leads to dissociation;[23] the most common explanation is that typically bound water has a slightly higher

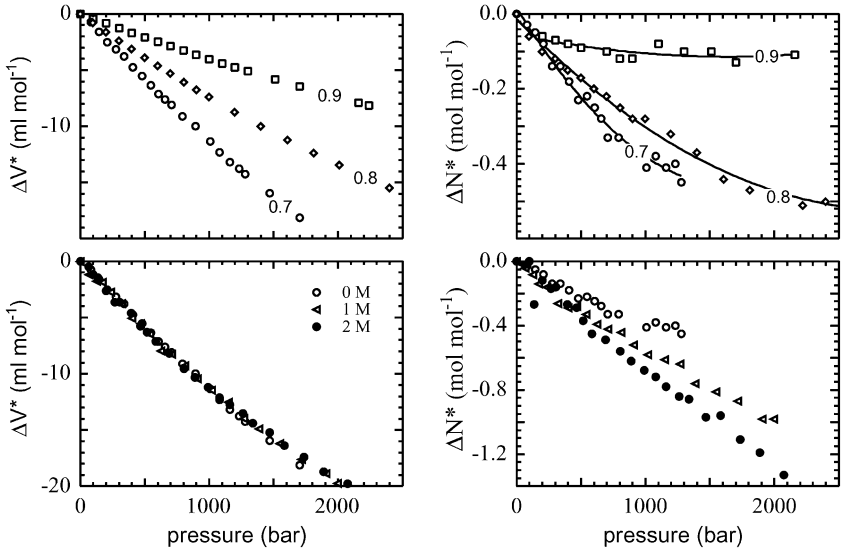


**Figure 8.** Pressure dependence of the unit cell volume changes, $\Delta V^*$ (left frames) and of the number of released water molecules, $\Delta N^*$ (right frames) per guanosine residue. Top frames refer to samples in pure water, and lower frames, to samples at $c = 0.7$ in different KCl solutions. Lines are guides for the eye.

density than bulk water[23,24] and then when the pressure is increased, the system tries to create more surface and therefore tends to dissociate. According to this mechanism, it has been argued that water close to the DNA bases has slightly lower density, so pressure favors better base stacking because of the water release and the consequent decrease in the system volume.[22]

We suggest that in GMP helices pressure will also favor base stacking because of the consequent decrease in the system volume. The first effect of better base stacking will be water release from the axial to the lateral interhelical region, but a related effect would be a release of counterions from the helix, which will also cause a negative volume change for the increased electrostriction of water.[16,21] According to the hydration force scheme,[13,25] a redistribution of bound counterions on the helix surface will affect the balance between repulsive and attractive lateral forces, and a net repulsion may then result from an unfavorable surface charge-distribution pattern. Moreover, the interhelix entropically favored attraction[26] is also expected to decrease as a function of pressure because the entropy difference of water near the charged helix surfaces and that of the bathing medium will be reduced by the increase in density of the bulk water. Because the fraction of water in the interhelix axial and lateral regions is dictated by the balance between repulsive and attractive contributions, we conclude that the observed anisotropic compressibilities reflect the dominating role of lateral forces on the interhelix equilibrium distance.

This picture also accounts for the larger water release observed when the ionic strength increases. The screening of the repulsive electrostatic forces determines at ambient pressure a redistribution of water from the lateral to the axial regions (the hexagonal cell decreases as a function of KCl): because of the reduced force strength, the opposite process then appears to be favored by compression. Within this oversimplified framework, it should be also taken into account that the sample volume is expected to depend on the charge of the helix (the volume ought to increase when the charge is removed[16]). However, the effective charge on the helix depends on the local ionic strength and pH of the bathing solution, which are in turn strongly related to the interaxial distance, so this process can hardly be discussed.

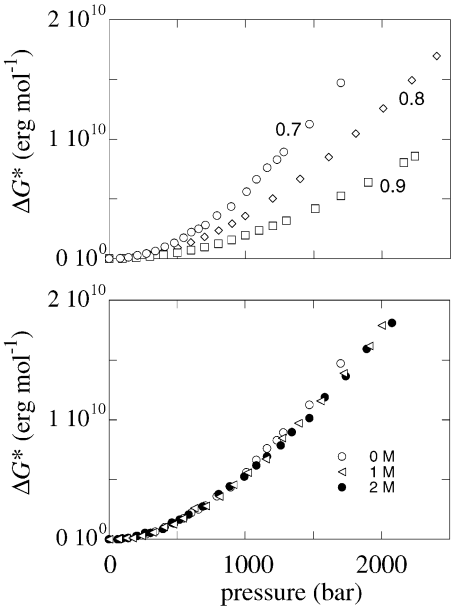


**Figure 9.** Pressure dependence of the total free energy per guanosine residue, $\Delta G^*$. Top frame, samples in pure water; lower frame, samples at $c = 0.7$ in different KCl solutions.

The energetic cost associated with the isothermal compression can be calculated by numerical integration of the external pressure $P$ over the cell volume $V_{cell}$. By definition,

$$\Delta G^* = -\frac{\aleph}{4n}\int P \, dV_{cell} \qquad (5)$$

where $\Delta G^*$ (erg mol$^{-1}$) is the change in free energy per guanosine residue. $\Delta G^*$ values, calculated using $n = 70$,[9,10] are shown in Figure 9 as a function of pressure. Noticeable are the dependence of $\Delta G^*$ on hydration (free-energy changes indeed include the work for transferring water molecules from the axial to the lateral interhelix regions), its independence of the ionic strength, and its magnitude, which is close to the strength of a typical van der Waals bond (about $10^{10}$ erg mol$^{-1}$; most hydrogen bonds lie between $10 \times 10^{10}$ and $40 \times 10^{10}$ erg mol$^{-1}$). Owing to the different mechanisms that account for the

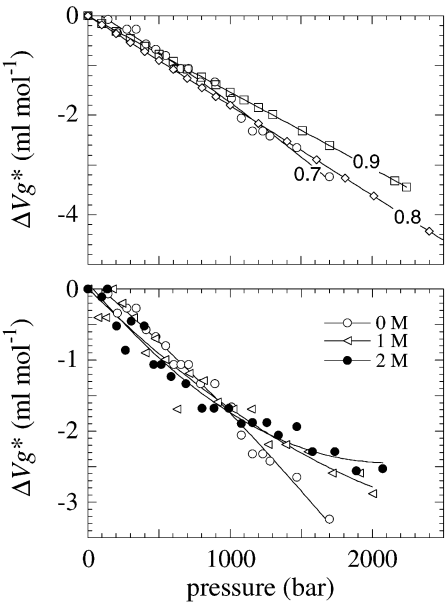


**Figure 10.** Pressure dependence of the partial volume changes of the GMP helices per guanosine residue, $\Delta V^*_g$. Top frame, samples in pure water; lower frame, samples at $c = 0.7$ in different KCl solutions. Lines are guides for the eye.

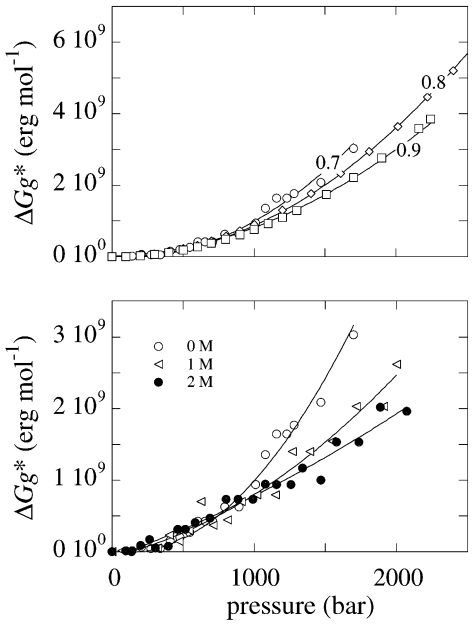


**Figure 11.** Changes in the free energy of the GMP helix per guanosine residue, $\Delta G_g^*$, during compression. Top frame, samples in pure water; lower frame, samples at $c = 0.7$ in different KCl solutions. Lines are best-fit curves obtained using equation 7. The fitting parameters are ($\kappa$ in dyne cm$^{-1}$, $b_0$ in Å) $c = 0.7$ and KCl 0 M, $\kappa = (3.85 \pm 0.07) \times 10^5$, $b_0 = 3.292 \pm 0.001$; $c = 0.8$ and KCl 0 M, $\kappa = (3.85 \pm 0.05) \times 10^5$, $b_0 = 3.282 \pm 0.001$; $c = 0.9$ and KCl 0 M, $\kappa = (3.85 \pm 0.08) \times 10^5$, $b_0 = 3.276 \pm 0.001$; $c = 0.7$ and KCl 1 M, $\kappa = (4.65 \pm 0.15) \times 10^5$, $b_0 = 3.321 \pm 0.001$; $c = 0.7$ and KCl 2 M, $\kappa = (4.69 \pm 0.18) \times 10^5$, $b_0 = 3.340 \pm 0.001$.

observed pressure effects and the extent to which they can contribute, it is not straightforward to derive inter- and intramolecular contributions to the free-energy changes. An analysis is reported in the following paragraph, but it should be clear that it is only tentative, being based on the questionable assumption that water has the same compressibility inside the hexagonal phase as in the bulk.

*Partial Volumetric Analysis.* To a first approximation, the net volume change $\Delta V$ (and $\Delta V^*$ in eq 3) can be written as a sum of two components:[21] the first is related to the helix structural properties, $\Delta V_g$ (and $\Delta V^*_g$), which includes the changes in the partial volume of the solute as well as any change in the interstitial volume owing to interactions of the solute with the solvent, and the second arises from changes in the partial volume of the water, $\Delta V_{wat}$ (and $\Delta V^*_{wat}$).

Because of differences in the hydrogen-bond networks in confined spaces, the compressibility of the water within the GMP phase is expected to be different from the compressibility in bulk water. However, because independent experimental data on the helix and on the water are hard to get, we are forced to make some assumptions about the contributions of these factors.[21,22] We will assume hereafter that the pressure dependence of the partial volume of the water within the hexagonal phase is the same as in bulk water, so $\Delta V_{wat}$ during compression can be easily determined from the literature (see for example ref 17). The helix volume change can then be obtained as a function of pressure by $\Delta V^*_g = \Delta V^* - \Delta V^*_{wat}$. Note that experimental results on the structure of the protein−water interface point to the existence of a first hydration shell with an average density that is 10% larger than that of the bulk water.[24] The comparisons with the results of other studies suggested that this may be a general property of aqueous interfaces.[27] We then expect that the difference in the average compressibility of water within the GMP hexagonal phase should be of the same order of magnitude, so the inaccuracy of the following results should not be larger than 10%.

Partial volume changes related to the GMP are reported in Figure 10; as expected, $\Delta V^*_g$ values are negative and depend neither on concentration nor on ionic strength. Moreover, GMP volume changes are very comparable to the 2 to 5 mL mol$^{-1}$ volume changes measured in DNA for the helix−coil transition (which mainly concerns the base stacking),[22] strongly confirming that a similar mechanism occurs (i.e., in both cases, pressure favors base stacking). Note also that the changes in ionic strength result in a small reduction of the helix volume at high pressure, in agreement with the observation that the presence of KCl increases the helix stiffness.

The calculated partial volume changes have then been used to separate the compression work into two components: the first is related to water, and the second, to guanosine helices. In particular, the second component has the form

$$\Delta G^*_g = -\frac{\aleph}{4n}\int P \, dV_g \qquad (6)$$

and its pressure dependence is reported in Figure 11. It can be observed that the helix compression work depends both on hydration and on ionic strength. In a first approximation, the observed changes in free energy can be expected to originate mainly from changes in interactions between adjacent base tetrads; the first term in the $\Delta G_g$ expansion is then related to the tetramer stacking distance. The classical form of the elastic energy of a spring has been used to describe the macroscopic cost to compress the GMP helix:

$$\Delta G_{el}^* = \frac{(n-1)\aleph}{8n}\kappa(b - b_0)^2 \qquad (7)$$

where $\kappa$ is the elastic constant (in dynes cm$^{-1}$), $n = 70$,[9,10] and $(n - 1)$ is the number of tetramer pairs. The best-fit curves obtained using eq 7 are shown in Figure 11. Describing the compression work only in terms of stacking elasticity is certainly a crude simplification, but a few comments can be useful. At

constant ionic strength, a unique elastic constant fits energy data obtained at different hydrations (in pure water, $\kappa = 3.85 \times 10^5$ dyne cm$^{-1}$, which corresponds to an elasticity Young's modulus of ~22 GPa and to a stretch modulus of $10^5$ pN), suggesting that stacking distances and the extent of stacking interactions are not explicitly correlated. More interesting, at constant concentration, the fitted $\kappa$ values confirm that KCl increases the helix rigidity. (At $c = 0.7$, $\kappa$ changes from $3.85 \times 10^5$ to $4.64 \times 10^5$ and $4.69 \times 10^5$ dyne cm$^{-1}$ when KCl increases from 0 to 1 and 2 M, respectively.) This fact can be reasonably related to the helix stabilization induced by counterions.[1,5,7]

It is interesting that the derived elastic constants are largely different from the mechanical constants measured in single-molecule DNA stretching experiments.[28] (Spring constants of $\sim 10^{-5}$ dyne cm$^{-1}$ have been measured in the DNA entropic elastic regime, and stretch moduli of $\sim 10^3$ pN have been observed in the linear elastic regime when the DNA molecule behaves as a stretchable solid.) However, forces involved in optical tweezers and atomic force microscopy investigations are quite different from compression forces applied in the present experiment, and the thermodynamic processes of compression/stretching are completely different in the two cases. Therefore, it appears that the range of forces determines the nature and length scale involved in the elastic response, with higher forces probing shorter length units. We are then persuaded that the reported experimental data might be helpful in using theoretical approaches in further analysis at different force/extension regimes.

**Acknowledgment.** P.M. acknowledges the financial support of INFM (Italy) and ESRF (France) within the framework of the Synchrotron Radiation project.

## References and Notes

(1) Gellert, M.; Lipsett, M. N.; Davies, D. R. *Proc. Natl. Acad. Sci. U.S.A.* **1962**, *48*, 2013.

(2) Saenger, W. *Principles of Nucleic Acid Structure*; Springer-Verlag: Heidelberg, Germany, 1984.

(3) Gottarelli, G.; Spada, G. P.; Mariani, P. In *Crystallography of Supramolecular Compounds*; Tsoucaris, G., Atwood, J. L., Lipkowski, J., Eds.; Kluwer Academic Publishers: Dordrecht, The Netherlands, 1996; p 307.

(4) Gibert, D. E.; Feigon, J. *Curr. Opin. Struct. Biology* **1999**, *9*, 305.

(5) Simonsson, T. *Biol. Chem.* **2001**, *382*, 621.

(6) Mergny, J.-L.; Jailliet, P.; Lavelle, F.; Riou, J. F.; Laoui, A.; Helene, C. *Anti-Cancer Drug Des.* **1999**, *14*, 327.

(7) Detellier, C.; Laszlo, P. *J. Am. Chem. Soc.* ***1980***, *102*, 1135.

(8) Amaral, L. Q.; Itri, R.; Mariani, P.; Micheletto, R. *Liq. Cryst.* **1992**, *12*, 913.

(9) Ausili, P.; Strey, H.; Mariani, P. Unpublished work.

(10) Mariani, P. Mazabard, C.; Garbesi, A.; Spada, G. P. *J. Am. Chem. Soc.* **1989**, *111*, 6369. Franz, H.; Ciuchi, F.; Di Nicola, G.; De Morais, M. M.; Mariani, P. *Phys. Rev. E* **1994**, *50*, 395. Gottarelli, G.; Proni, G.; Spada, G. P.; Bonazzi, S.; Garbesi, A.; Ciuchi, F.; Mariani, P. *Bioploymers* **1997**, *42*, 561.

(11) Kornyshev, A. A.; Leikin, S. *Proc. Natl. Acad. Sci. U.S.A.* **1998**, *95*, 13579. Kornyshev, A. A.; Leikin, S. *Proc. Natl. Acad. Sci. U.S.A.* **2001**, *86*, 3666. Kornyshev, A. A.; Leikin, S. *Phys. Rev. E* **2000**, *62*, 2576. Harreis, H. M.; Kornyshev, A. A.; Likos, C. N.; Lowen, H.; Sutmann, G. *Phys. Rev. Lett.* **2002**, *89*, 18303. Cherstvy, A.; Kornyshev, A. A.; Leikin, S. *J. Phys. Chem. B* **2002**, *106*, 13362. Lorman, V.; Podgornik, R.; Zeks, B. *Phys. Rev. Lett.* **2001**, *87*, 218101. Hansen, P. L.; Podgornik, R.; Parsegian, V. A. *Phys. Rev. E* **2001**, *64*, 021907.

(12) Strey, H. H.; Parsegian, V. A.; Podgornik, R. *Phys. Rev. E*, **1999**, *59*, 999. Ha, B.-Y.; Liu, A. J. *Phys. Rev. E* **1999**, *60*, 803. Kornyshev, A. A.; Leikin, S. *Biophys. J.* **1998**, *75*, 2513. Kornyshev, A. A.; Leikin, S. *Phys. Rev. Lett.* **2000**, *84*, 2537.

(13) Mariani, P.; Saturni, L. *Biophys. J.* **1996**, *70*, 2867. Mariani, P.; Ciuchi, F.; Saturni, L. *Biophys. J.* **1998**, *72*, 2867.

(14) Ausili, P. Ph.D. Thesis, Ancona University, 2002.

(15) Winter, R. *Curr. Opin. Colloid Interface Sci.* **2001**, *6*, 303. Winter, R. *Biochim. Biophys. Acta* **2002**, *36562*, 1.

(16) Macgregor, R. B.; Wu, J. Q.; Najaf-Zadeh, R. In *High-Pressure Effects in Molecular Biophysics and Enzymology*; Markley, J. L., Northrop, D. B., Royer, C. A., Eds.; Oxford University Press: Oxford, England, 1996; p 149. Lin, M.-C.; Macgregor, R. B. *Biochemistry* **1997**, *35*, 6539.

(17) *Roark's Formulas for Stress & Strain*, 6th ed.; Young, W. C., Ed.; McGraw-Hill: New York, 1989.

(18) Pisani, M. Ph.D. Thesis, Ancona University, 2001.

(19) Pisani, M.; Bernstorff, S.; Ferrero, C.; Mariani, P. *J. Chem. Phys. B* **2001**, *54*, 5840.

(20) Pisani, M.; Narayanan, T.; Di Gregorio, G. M.; Ferrero, C.; Finet, S.; Mariani, P. *Phys. Rev. E* **2003**, *68*, 21924.

(21) Prehoda, K. E.; Markley, J. L. In *High-Pressure Effects in Molecular Biophysics and Enzymology*; Markley, J. L., Northrop, D. B., Royer, C. A., Eds.; Oxford University Press: Oxford, England, 1996; p 33.

(22) Balny, C.; Masson, P.; Heremans, K. *Biochim. Biophys. Acta* **2002**, *1595*, 3.

(23) Silva, J. L.; Foguel, D.; Da Poian, A. T.; Prevelige, P. E. *Curr. Opin. Struct. Biol.* **1996**, *6*, 166. Heremans, K.; Smeller, L. In *Biological Systems Under Extreme Conditions*; Taniguchi, Y., Stanley, H. E., Ludwig, H., Eds.; Springer-Verlag: Berlin, 2002; p 53.

(24) Svergun, D. I.; Richard, S.; Koch, M. H.; Sayers, Z.; Kuprin, S.; Zaccai, G. *Proc. Natl. Acad. Sci. U.S.A.* **1998**, *95*, 2267.

(25) Leikin, S.; Kornyshev, A. A. *Phys. Rev. A* **1991**, *44*, 1156. Leikin, S.; Rau, D. C.; Parsegian, V. A. *Proc. Natl. Acad. Sci. U.S.A.* **1994**, *91*, 276. Kornyshev, A. A.; Leikin, S. *J. Chem. Phys.* **1997**, *107*, 3656. Kornyshev, A. A.; Leikin, S. *J. Chem. Phys.* **1998**, *108*, 7035.

(26) Rau, D. C.; Parsegian, V. A. *Biophys. J.* **1992**, *61*, 260.

(27) Toney, M. F.; Howard, J. N.; Richer, J.; Borges, G. L.; Gordon, J. G.; Melroy, O. R.; Wiesler, D. G.; Yee, D.; Sorensen, L. B. *Nature (London)* **1994**, *368*, 444.

(28) Bustamante, C.; Smith, S. B.; Liphardt, J.; Smith, D. *Curr. Opin. Struct. Biol.* **2000**, *10*, 279.